Nitrogen Use Efficiency Is Mediated by Vacuolar Nitrate Sequestration Capacity in Roots of *Brassica napus*[OPEN]

Yong-Liang Han[1], Hai-Xing Song[1], Qiong Liao[1], Yin Yu[1], Shao-Fen Jian[1], Joe Eugene Lepo, Qiang Liu, Xiang-Min Rong, Chang Tian, Jing Zeng, Chun-Yun Guan, Abdelbagi M. Ismail, and Zhen-Hua Zhang*

Southern Regional Collaborative Innovation Center for Grain and Oil Crops in China, Hunan Agricultural University, Changsha, 410128, China (Y.-L.H., H.-X.S., Q.Liao, Y.Y., S.-F.J., Q.Liu, X.-M.R., C.T., J.Z., C.-Y.G., Z.-H.Z.); National Center of Oilseed Crops Improvement, Hunan Branch, Changsha, 410128, China (C.-Y.G.); Center for Environmental Diagnostics and Bioremediation, University of West Florida, Pensacola, Florida 32514, (J.E.L.); and Crop and Environment Sciences Division, International Rice Research Institute, DAPO 7777, Metro Manila, Philippines (A.M.I.)

ORCID IDs: 0000-0002-7553-642X (S.-F.J.); 0000-0002-1961-3072 (A.M.I.).

Enhancing nitrogen use efficiency (NUE) in crop plants is an important breeding target to reduce excessive use of chemical fertilizers, with substantial benefits to farmers and the environment. In Arabidopsis (*Arabidopsis thaliana*), allocation of more NO_3^- to shoots was associated with higher NUE; however, the commonality of this process across plant species have not been sufficiently studied. Two *Brassica napus* genotypes were identified with high and low NUE. We found that activities of V-ATPase and V-PPase, the two tonoplast proton-pumps, were significantly lower in roots of the high-NUE genotype (Xiangyou15) than in the low-NUE genotype (814); and consequently, less vacuolar NO_3^- was retained in roots of Xiangyou15. Moreover, NO_3^- concentration in xylem sap, [^{15}N] shoot:root (S:R) and [NO_3^-] S:R ratios were significantly higher in Xiangyou15. *BnNRT1.5* expression was higher in roots of Xiangyou15 compared with 814, while *BnNRT1.8* expression was lower. In both *B. napus* treated with proton pump inhibitors or Arabidopsis mutants impaired in proton pump activity, vacuolar sequestration capacity (VSC) of NO_3^- in roots substantially decreased. Expression of *NRT1.5* was up-regulated, but *NRT1.8* was down-regulated, driving greater NO_3^- long-distance transport from roots to shoots. NUE in Arabidopsis mutants impaired in proton pumps was also significantly higher than in the wild type col-0. Taken together, these data suggest that decrease in VSC of NO_3^- in roots will enhance transport to shoot and essentially contribute to higher NUE by promoting NO_3^- allocation to aerial parts, likely through coordinated regulation of *NRT1.5* and *NRT1.8*.

China is the largest consumer of nitrogen (N) fertilizer in the world; however, the average N use efficiency (NUE) in fertilizer is only around 35%, suggesting considerable potential for improvements (Shen et al., 2003; Wang et al., 2014). With the high amounts of N-fertilizer being used, crop yields are declining in some areas, where application is exceeding the optimum required for local field crops (Shen et al., 2003; Miller and Smith, 2008; Xu et al., 2012). The extremely low NUE results in waste of resources and environmental contamination, and also presents serious hazards for human health (Xu et al., 2012; Chen et al., 2014). Consequently, exploiting the maximum potential for improving NUE in crop plants will have practical significance for agriculture production and the environment (Zhang et al., 2010; Schroeder et al., 2013; Wang et al., 2014). Elucidating the genetic and physiological regulatory mechanisms governing NUE in plants will allow breeding crops and varieties with higher NUE.

Ammonium (NH_4^+) and nitrate (NO_3^-) are the main N species absorbed and utilized by crops, and NO_3^- accumulation and utilization are of major emphasis for N nutrient studies in dry land crops, such as *Brassica napus*. Several studies revealed the close relationship between NO_3^- content and NUE in plant tissues (Shen et al., 2003; Zhang et al., 2012; Tang et al., 2013; Han et al., 2015a). When plants are sufficiently illuminated, NO_3^- assimilation efficiency significantly increase in shoots compared with roots (Smirnoff and Stewart,

[1] These authors contributed equally to this work.

* Address correspondence to zhzh1468@163.com.

The author responsible for distribution of materials integral to the findings presented in this article in accordance with the policy described in the Instructions for Authors (www.plantphysiol.org) is: Zhen-Hua Zhang (zhzh1468@163.com).

This study was supported by the National Natural Science Foundation of China (Grant No.31101596, 31372130); Hunan Provincial Recruitment Program of Foreign Experts; National Oilseed Rape Production Technology System of China; "2011 Plan" supported by The Ministry of Education in China; Open Novel Science Foundation of Hunan province (13K062). National Key Laboratory of Plant Molecular Genetics and the "Twelfth Five-Year" National Science and technology support program (2012BAD15BO4).

Z.-H.Z. conceived the original screening and research plans; Z.-H.Z. supervised the experiments; Y.-L.H., H.-X.S., Q.L., Y.Y., S.-F.J., and Z.-H.Z. performed most of the experiments; C.T. and J.Z. provided technical assistance to Y.-L.H., H.-X.S., Y.Y., and Z.-H.Z.; Y.-L.H., and Z.-H.Z. designed the experiments and analyzed the data; Q.L., X.-M.R., C.-Y.G., and Z.-H.Z. interpreted the results and J.E.L., A.I., and Z.-H.Z. conceived the project and wrote the article with contributions of all the authors; J.E.L., A.I. and Z.-H.Z. supervised and complemented the writing. All authors read and approved the final manuscript.

[OPEN] Articles can be viewed without a subscription.

www.plantphysiol.org/cgi/doi/10.1104/pp.15.01377

1985; Tang et al., 2013). Consequently, under daytime with optimal illumination, higher proportion of NO_3^- in plant tissue is transported from root to shoot, as an advantageous physiological adaptation that reduces the cost of energy for metabolism (Tang et al., 2013). NO_3^- assimilation in plant shoots can therefore take advantage of solar energy while improving NUE (Smirnoff and Stewart, 1985; Andrews, 1986; Tang et al., 2012, 2013).

The NO_3^- long-distance transport and distribution between root and shoot is regulated by two genes encoding long transport mechanisms. *NRT1.5* is responsible for xylem NO_3^- loading, while *NRT1.8* is responsible for xylem NO_3^- unloading (Lin et al., 2008; Li et al., 2010). Expression of the two genes is influenced by NO_3^- concentration. *NRT1.5* is strongly induced by NO_3^- (Lin et al., 2008), while *NRT1.8* expression is extremely up-regulated in *nrt1.5* mutants (Chen et al., 2012). A negative correlation between the extents of expression of the two genes was observed when plants are subjected to abiotic stresses (Chen et al., 2012). Moreover, expression of *NRT1.5* is strongly inhibited by 1-aminocyclopropane-1-carboxylic acid (ACC) and methyl jasmonate (MeJA), whereas the expression of *NRT1.8* is significantly up-regulated (Zhang et al., 2014). Based on these studies, we argue that the expression and functioning of NO_3^- long-distance transport genes *NRT1.5* and *NRT1.8* are regulated by cytosolic NO_3^- concentration. In addition, the vacuolar and cytosolic NO_3^- distribution is likely regulated by proton pumps located within the tonoplast (V-ATPase and V-PPase; Granstedt and Huffaker, 1982; Glass et al., 2002; Krebs et al., 2010). Therefore, NO_3^- use efficiency must be affected by NO_3^- long-distant transport (between shoot and root) and short-distant transport (between vacuole and cytosol). However, the physiological mechanisms controlling this regulation are still obscure.

Previous studies showed that the chloride channel protein (CLCa) is mainly responsible for vacuole NO_3^- short-distance transport, as it is the main channel for NO_3^- movement between the vacuoles and cytosol (De Angeli et al., 2006; Wege et al., 2014). The vacuole proton-pumps (V-ATPase and V-PPase) located in the tonoplast supply energy for active transport of NO_3^- and accumulation within the vacuole (Gaxiola et al., 2001; Brüx et al., 2008; Krebs et al., 2010). Despite the fact about 90% of the volume of mature plant cells is occupied by vacuoles, vacuolar NO_3^- cannot be efficiently assimilated because the enzyme nitrate reductase (NR) is cytosolic (Shen et al., 2003; Han et al., 2015a). However, retranslocation of NO_3^- from the vacuole to the cytosol will permit its immediate assimilation and utilization.

Generally, NO_3^- concentrations in plant cell vacuoles and the cytoplasm are in the range of 30–50 mol m^{-3} and 3–5 mol m^{-3}, respectively (Martinoia et al., 1981, 2000). Because vacuoles are obviously the organelle for high NO_3^- accumulation and storage in plant tissues, their function in NO_3^- use efficiency cannot be ignored (Martinoia et al., 1981; Zhang et al., 2012; Han et al., 2015b). NO_3^- assimilatory system in the cytoplasm is sufficient for its assimilation when it is transported out of the vacuoles. Therefore, NO_3^- use efficiency could in part be dependent on vacuolar-cytosolic NO_3^- short-distance transport in plant tissues (Martinoia et al., 1981; Shen et al., 2003; Zhang et al., 2012; Han et al., 2015a).

Evidently, NO_3^- use efficiency is regulated by both NO_3^- long-distance transport from root to shoot and short-distance transport and distribution between vacuoles and cytoplasm within cells (Glass et al., 2002; Dechorgnat et al., 2011; Han et al., 2015a). Although vacuoles compartment excess NO_3^- that accumulates in plant cells (Granstedt and Huffaker, 1982; Krebs et al., 2010), neither NO_3^- inducible NR genes (*NIA1* and *NIA2*; Fan et al., 2007; Han et al., 2015a) nor the NO_3^- long-distance transport gene *NRT1.5* (Lin et al., 2008) are regulated by vacuolar NO_3^-, even though they are essential for NO_3^- assimilation. Only NO_3^- transported from the vacuole to the cytosol can play a role in regulating NO_3^- inducible genes. Consequently, we argue that both NO_3^- assimilation in cells and its long-distance transport from root to shoot are regulated by cytosolic NO_3^- concentration. However, this hypothesis needs to be substantiated. The mechanisms underlying both NO_3^- short-distance (Gaxiola et al., 2001; De Angeli et al., 2006; Brüx et al., 2008; Krebs et al., 2010) and long-distance transport (Lin et al., 2008; Li et al., 2010) have been previously investigated, yet the underlying mechanisms regulating the flux of NO_3^- and the obvious relationship between the two transport pathways, as well as their relation to NUE, are not well understood.

The *NRT* family of genes play a partial role in vacuolar NO_3^- accumulation in petioles (Chiu et al., 2004) and seed tissues (Chopin et al., 2007), whereas the proton pumps and CLCa system in the tonoplast play a major role in accumulating NO_3^- in vacuoles (Gaxiola et al., 2001; De Angeli et al., 2006; Brüx et al., 2008; Krebs et al., 2010). The vacuolar NO_3^- short-distance transport system is spread throughout the plant tissues and is the principal means by which vacuolar NO_3^- short-distance transport and distribution is controlled (De Angeli et al., 2006; Krebs et al., 2010).

The *NRT* genes seem to work synergistically to control NO_3^- long-distance transport between roots and shoots. *NRT1.9* is responsible for NO_3^- loading into the phloem (Wang and Tsay, 2011), whereas NO_3^- loading and unloading into xylem are regulated by *NRT1.5* and *NRT1.8*, respectively (Lin et al., 2008; Li et al.; 2010). Phloem transport mainly involves organic N; the inorganic-N (NO_3^-) concentrations in the phloem sap are typically very low, ranging from one-tenth to one-hundredth of that of the inorganic-N in xylem sap (Lin et al., 2008; Fan et al., 2009). Therefore, this study focused on NO_3^- short-distance transport mediated through the tonoplast proton pumps and the CLCa system and the long-distant transport mechanisms responsible for xylem NO_3^- loading and unloading via *NRT1.5* and *NRT1.8*, respectively.

Questions related to how long- and short-distance transport of NO_3^- are coupled in plant tissues and their role in determining NUE were addressed using a pair of high- and low-NUE *B. napus* genotypes and Arabidopsis (*Arabidopsis thaliana*). Application of proton pump inhibitors and ACC in the former, and use of mutants with defective proton pumps in the latter, allowed experimental distinction of the physiological mechanisms regulating these processes. Data presented here provide strong evidence from both model plants supporting this linkage and strongly suggest that cytosolic NO_3^- concentration in roots regulates NO_3^- long-distance transport from roots to shoots. We also investigated how NO_3^- concentration in plant tissues would be affected by NO_3^- long-distance transport, vacuolar NO_3^- sequestration, and the ensuing relationship with NO_3^- use efficiency. We also proposed the physiological mechanisms likely to be important for enhancing NO_3^- use efficiency in plants. These findings will provide scientific rationales for improving NUE in important industrial and food crops.

RESULTS

B. napus with Higher NUE Showed Lower Vacuolar Sequestration Capacity for NO_3^- in Root Tissues

Our previous work identified high and low NUE *B. napus* genotypes (Han et al., 2015a; Han et al., 2015b). NUE of *B. napus*, whether based on biomass or on grain yield (Table I), was significantly higher for the high-NUE genotype (H: Xiangyou15) than for the low-NUE genotype (L: 814). The activities of the tonoplast proton pumps (V-ATPase and V-PPase) of root tissues in the H genotype were lower than the L genotype at both seedling (Fig. 1A) and flowering stages (Supplemental Fig. S1A). Given that proton pumps in the tonoplast supply energy for vacuolar NO_3^- accumulation (Krebs et al., 2010), NO_3^- influx into the vacuole was consequently much slower in the H genotype compared with the L genotype at both seedling (Fig. 1B) and flowering stages (Supplemental Fig. S1B). Moreover, the percentage of vacuolar NO_3^- relative to the total NO_3^- in protoplasts of root tissues in the H genotype was lower than in the L genotype at seedling (Fig. 1C) and flowering stages (Supplemental Fig. S1C), and NO_3^- accumulation in the cytosol increased significantly in the H genotype compared with the L genotype at seedling (Fig. 1D) and flowering stages (Supplemental Fig. S1D).

B. napus with Higher NUE Showed Enhanced Long-Distance Transport of NO_3^- from Roots to Shoots

The relative expression of *BnNRT1.5* in roots of the H genotype was significantly higher than that in the L genotype at both seedling and flowering stages, while the relative expression of *BnNRT1.8* in roots of the H genotype was lower than that in the L genotype at both seedling (Fig. 2, A and B) and flowering stages (Supplemental Fig. S2, A and B). As a consequence, total N concentration (traced by ^{15}N) in roots of the H genotype was significantly lower than that of the L genotype at both seedling (Fig. 2C) and flowering stages (Supplemental Fig. S2C), while shoot N concentration in the H genotype was significantly higher than the L genotype at seedling stage (Fig. 2C). This resulted in significantly higher [^{15}N] S:R ratio in the H genotype compared with the L genotype (Fig. 2D; Supplemental Fig. S2D).

No significant differences in total N per plant between the H and L genotypes were observed at both seedling and flowering stages (Supplemental Fig. S3). However, NO_3^- concentration in roots of the H genotype was significantly lower than in the L genotype at both seedling and flowering stages (Fig. 2E; Supplemental Fig. S2E), while NO_3^- concentration in shoot tissues of this genotype was significantly higher at seedling stage (Fig. 2E), resulting in higher [NO_3^-] S:R ratios at both stages (Fig. 2F; Supplemental Fig. S2F).

NO_3^- concentration in the xylem sap, xylem sap volume, and total NO_3^- in xylem sap were significantly higher in the H genotype than in the L genotype at seedling stage (Supplemental Fig. S4, A, C, and E); the amount of NO_3^- in xylem sap significantly increased in the H genotype relative to the L genotype at flowering stage (Supplemental Fig. S4F). Together, these data suggest greater mobilization of NO_3^- from root to shoot in the H genotype.

NO_3^- Up-Regulates *NRT1.5*, but Down-Regulates *NRT1.8*

A previous study showed that increased *NRT1.8* expression in *nrt1.5* mutants (Chen et al., 2012) and the expression of *NRT1.5* was induced by NO_3^- (Lin et al., 2008). We tested the relationship between *NRT1.5* and *NRT1.8* expression in Arabidopsis and *B. napus*. No significant differences were observed in *AtNRT1.5* expression in roots between wild type (col-0) and mutant plants (*nrt1.8-2*; Fig. 3A). However, *AtNRT1.5* expression

Table I. *Comparison of NUE between the two B. napus genotype*

Different letters associated with data represent significant differences at $P < 0.05$, $n = 3$.

[b]Genotypes	Biomass (g plant^{-1})	Physiological parameters		[a]NUE	
		Grain yield (g plant^{-1})	Total N in plant (g plant^{-1})	Based on biomass (gg^{-1})	Based on grain yield (gg^{-1})
H	139.44 ± 6.77a	31.26 ± 0.50a	2.61 ± 0.08a	53.54 ± 2.40a	12.01 ± 0.44a
L	108.73 ± 3.05b	20.84 ± 1.44b	2.45 ± 0.15a	44.40 ± 2.64b	8.53 ± 1.08b

[a]NUE values were calculated based on either total biomass (shoot, root and grains) per total N uptake or as grain yield per total N uptake. [b]H represents the high NUE genotype (Xiangyou15), and L represents the low NUE genotype (814).

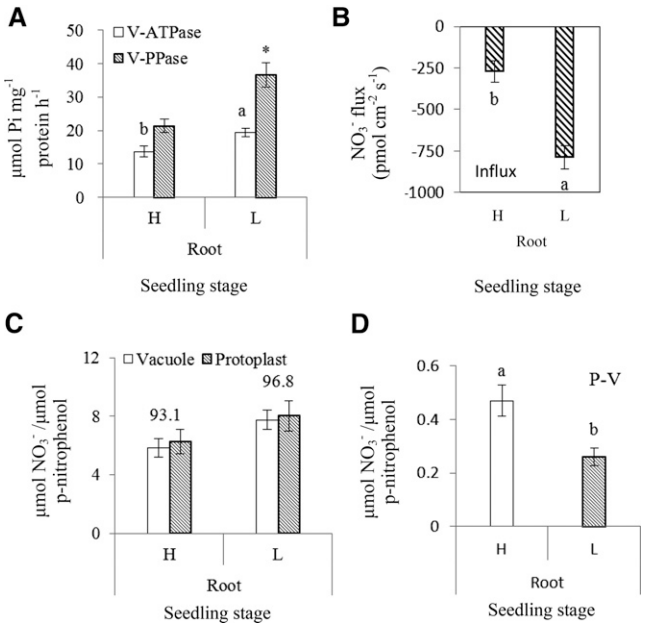

Figure 1. *B. napus* with higher NUE showed lower VSC for NO_3^- in roots at the seedling stage. H refers to the high-NUE oilseed rape genotype Xiangyou15 and L refers to the low-NUE genotype 814. Specific activities of the tonoplast proton pumps are expressed as μmol Pi released mg^{-1} protein h^{-1}. NO_3^- fluxes are expressed as pmol NO_3^- cm^{-2} S^{-1}. Mature vacuoles were collected from the root tissues at seedling stage and a microelectrode was vibrated in the measuring solution between the two positions 1 μm and 11 μm from the vacuole surface (tonoplast) along an axis perpendicular to the tangent of the target vacuoles recording the stable reading data. The background was recorded by vibrating the electrode in measuring solution without vacuoles. Protoplasts and vacuoles isolated from roots of hydroponically grown plants were measured for NO_3^- content and NO_3^- accumulation normalized against the specific activity of the vacuole acid phosphatase (ACP) as described in "Materials and Methods"; and plotted as μmol NO_3^- per μmol *p*-nitrophenol, the end product of ACP assay. Proton pump activities in root tissues between H and L genotypes are shown at the seedling stage (A). Different letters at the top of the histogram bars denote significant differences of V-ATPase in root tissues between H and L genotypes ($P < 0.05$); an asterisk (*) at the top of the histogram bars indicates significant difference in V-PPase activity in root tissues between H and L genotypes ($P < 0.05$). Vertical bars on the figures indicate SD ($n = 6$). Mean rates of NO_3^- flux during 160 s within vacuoles of root tissues between H and L genotypes are shown at the seedling stage (B). Different letters at the top of the histogram bars denote significant differences of NO_3^- flux between H and L genotypes ($P < 0.05$). Vertical bars on the figures indicate SD ($n = 6$). Accumulation of NO_3^- inside the vacuole and in the protoplasts of root tissues is shown at the seedling stage (C). Values above the bars represent the percentage of vacuolar NO_3^- relative to the total NO_3^- in protoplasts. NO_3^- accumulation in the cytosol of root tissues is shown at seedling stage (D). P-V is the total NO_3^- in the cytosol and was calculated a tostal NO_3^- in protoplasts – total NO_3^- in vacuole. Different letters at the top of histogram bars denote significant differences of total NO_3^- in cytosol between H and L genotypes ($P < 0.05$). Vertical bars on the figures indicate SD ($n = 6$).

was significantly up-regulated by NO_3^- in roots of *nrt1.8-2* mutants (Fig. 3B). Expression of *AtNRT1.8* significantly increased in roots of *nrt1.5-3* mutants, but not in col-0 plants, and there were no significant differences in *AtNRT1.8* expression with or without NO_3^- treatment in roots of *nrt1.5-3* mutants (Fig. 3, C and D).

In contrast, *BnNRT1.5* expression in roots of the H genotype increased significantly with NO_3^- treatment (Fig. 3E), while the reverse was observed in expression of *BnNRT1.8*, which showed lower expression under NO_3^- treatment than control (Fig. 3F).

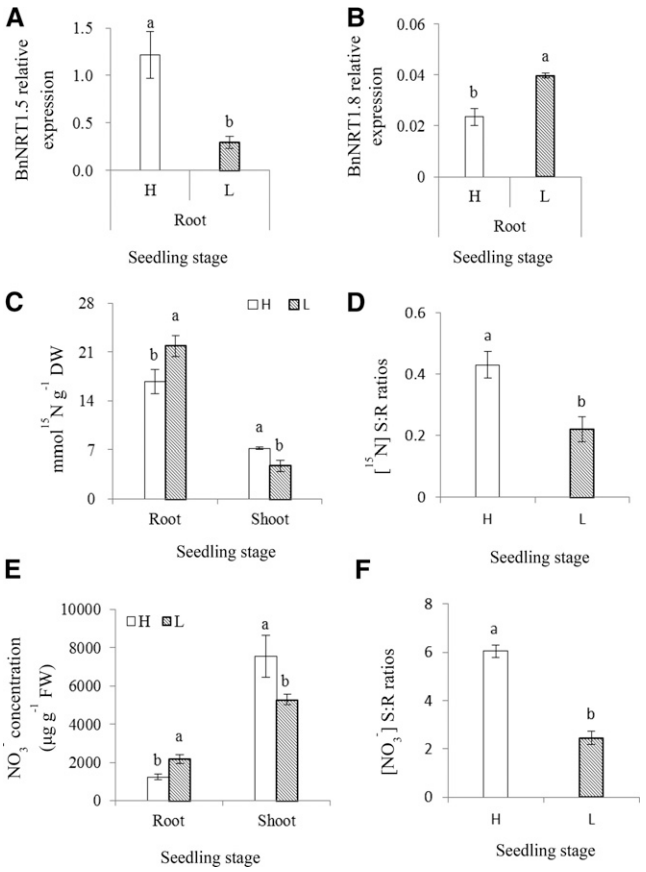

Figure 2. *B. napus* with higher NUE showed enhanced long-distance transport of NO_3^- from roots to shoots at the seedling stage. H refers to the high-NUE genotype Xiangyou15 and L refers to the low-NUE genotype 814. Expression of the *BnNRT1.5* (A) and *BnNRT1.8* (B) genes relative to that of the actin gene in the root tissues of the two genotypes at seedling stage was assessed by quantitative RT-PCR as described in "Materials and Methods"; a value of 1.0 is equivalent to levels of expression of the *Bnactin* gene. Vertical bars on the figures indicate SD ($n = 3$); different letters at the top of the histogram bars denote significant differences at $P < 0.05$. Hydroponically grown *B. napus* plants were subjected to ^{15}N-labeling treatment as described in "Materials and Methods." The ^{15}N concentration in the root and shoot tissues of the two genotypes is shown at the seedling stage (C). The [^{15}N] S:R ratios in the root and shoot tissues of the two genotypes are shown at the seedling stage (D).Vertical bars on the figures indicate SD ($n = 3$), different letters at the top of the histogram bars denote significant differences at $P < 0.05$ level. The NO_3^- concentration ($\mu g\ g^{-1}$ FW) in root and shoot tissues of the two genotypes are shown at the seedling stage (E). The [NO_3^-] S:R ratios in the root and shoot tissues of the two genotypes are shown at the seedling stage (F). Vertical bars on the figures indicate SD ($n = 3$), different letters at the top of the histogram bars denote significant differences at $P < 0.05$.

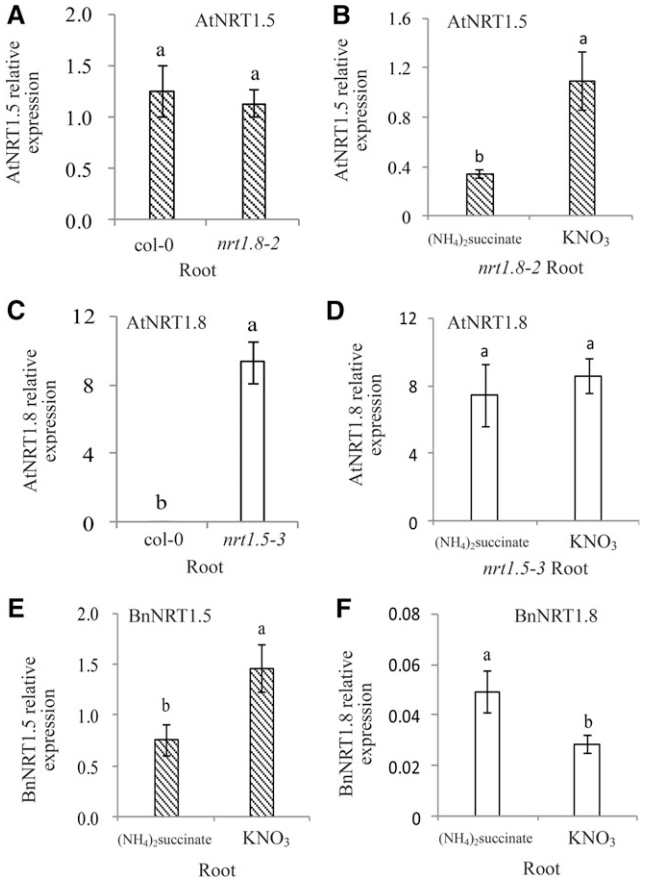

Figure 3. *NRT1.5* gene expression is up-regulated by NO_3^- and might affect downstream regulation of the *NRT1.8* gene. Culture conditions and plant materials are defined in the "Materials and Methods." Seedling stage Arabidopsis mutant plants (*nrt1.8-2* and *nrt1.5-3*) were cultured hydroponically with 2.25 mM $(NH_4)_2$ succinate for 3 d and shifted to hydroponics with 4.5 mM NO_3^- for 12 h, after which root tissues were collected for analysis. Expression of *AtNRT1.5* or *AtNRT1.8* genes were assessed by quantitative RT-PCR as described in "Materials and Methods" and presented relative to that of the *Atactin2* gene. *B. napus* (Xiangyou15) was cultured in hydroponics with 7.5 mM $(NH_4)_2$succinate for 3 d and shifted to hydroponics with 15 mM NO_3^- for 12 h, after which root tissues were collected for analysis as described in the "Materials and Methods." Relative expressions of the *AtNRT1.5* genes are shown at the seedling stage in root tissues of col-0 and *nrt1.8-2* (A). Relative expression of the *AtNRT1.5* gene is shown in root tissues of *nrt1.8-2* plants treated with either $(NH_4)_2$succinate for 3 d or shifted to hydroponics with NO_3^- for 12 h at the seedling stage (B). Relative expressions of the *AtNRT1.8* genes are shown at the seedling stage in root tissues of col-0 and *nrt1.5-3* (C). D shows results for the relative expression of the *AtNRT1.8* genes under the same conditions as in B. Relative expression of *BnNRT1.5* (E) and *BnNRT1.8* (F) genes in root tissues of *B. napus* (Xiangyou15) are shown at the seedling stage. Different letters at the top of the histogram bars denote significant differences ($P < 0.05$). Vertical bars on the figures indicate SD ($n = 6$).

This suggests that NO_3^- induces the expression of *NRT1.5*, but down-regulates *NRT1.8* in Arabidopsis and *B. napus*. Further studies are needed to elucidate the mechanisms regulating this reverse regulation.

Reduced Vacuolar Sequestration Capacity of NO_3^- in Roots Drives Its Long-Distance Transport from Roots to Shoots

Our previous study showed that Bafi (Bafilomycin A_1) inhibits V-ATPase; DCCD (DCCD + Na_2SO_3) inhibits V-PPase; and a 1:1 combination of Bafi and DCCD (B+D) inhibits both V-ATPase and V-PPase (Han et al., 2015a). These inhibitors were used to control activities of the tonoplast proton pumps in the H *B. napus* plants. V-ATPase activity significantly decreased under Bafil and B+D treatments relative to the control and DCCD treatments, whereas V-PPase activity declined significantly under DCCD and B+D treatments relative to that in the control and Bafil treatments (Fig. 4A).

The V-ATPase activity in roots of Arabidopsis was significantly lower in the V-ATPase mutants (*vha-a2* and *vha-a3*) than the wild type (col-0) and V-PPase mutants (*avp1*; Fig. 5A). In contrast, the V-PPase activity in roots of V-PPase mutant (*avp1*) were significantly lower than in the wild type (col-0) and V-ATPase mutants (*vha-a2* and *vha-a3*; Fig. 5A).

NO_3^- influxes into vacuoles of the H *B. napus* plants significantly decreased when treated with inhibitors of proton pumps (Bafil, DCCD, B+D; Fig. 4B). Similarly, NO_3^- influxes into the vacuole of the Arabidopsis mutants (*vha-a2*, *vha-a3*, and *avp1*) was significantly lower than those found in the wild type (col-0; Fig. 5B). Previous studies showed that vascular sequestration capacity (VSC) of NO_3^- decreased when the activities of the proton pumps decline (Li et al., 2005; Krebs et al., 2010; Han et al., 2015a).

We further investigated NO_3^- distribution between the vacuole and cytosol as affected by proton pump inhibition in the H genotype of *B. napus* and the mutants of Arabidopsis defective in vacuolar proton pumps. The percentage of vacuolar NO_3^- relative to total NO_3^- in root protoplasts of the H genotype treated with inhibitors (Bafil, DCCD, B+D) was lower than that observed in the control (Fig. 4C). Results were also similar when using Arabidopsis mutants, where the percentage of vacuolar NO_3^- relative to the total NO_3^- in protoplasts was lower in the mutants (*vha-a2*, *vha-a3*, and *avp1*) than in the wild type (col-0, Fig. 5C). Consequently, NO_3^- accumulation in the cytosol showed a significant increase when energy pumps were suppressed in roots of the H genotype (Fig. 4D), and NO_3^- accumulation in the cytosol of root tissues of Arabidopsis mutants (*vha-a2*, *vha-a3*, and *avp1*) similarly increased, compared with col-0 (Fig. 5D).

Based on previous observations (Lin et al., 2008), expression of *NRT1.5* is strongly induced by NO_3^-, but expression of *NRT1.8* is down-regulated (Fig. 3; Chen et al., 2012). We then hypothesized that expression of these two genes is contrastingly regulated by concentration of NO_3^- in the cytosol. Our results were congruent with this hypothesis: the expression of *BnNRT1.5* in root tissues of the H genotype of *B. napus* was significantly higher in plants treated with Bafil, DCCD or B+D, compared with the control (Fig. 4E), whereas the expression of

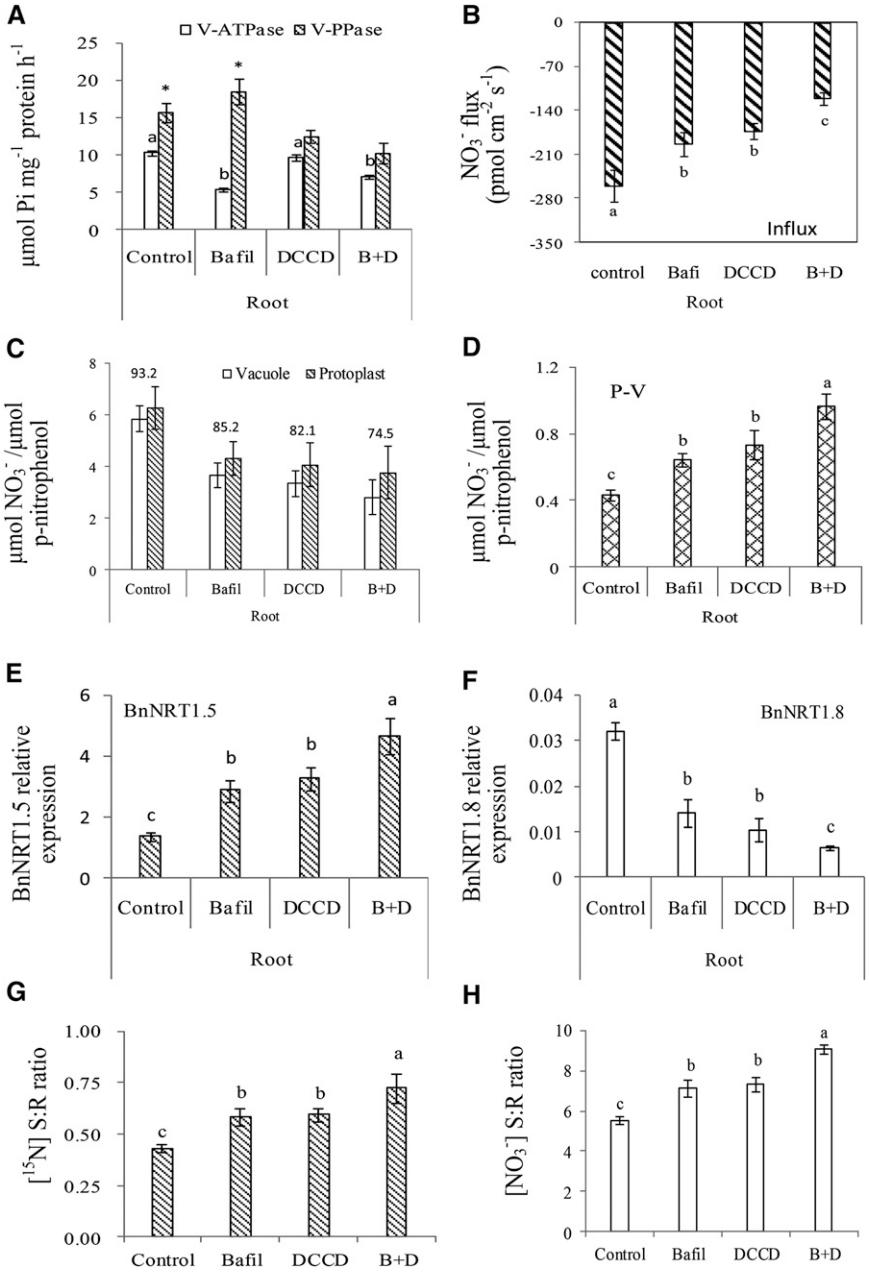

Figure 4. Reduced VSC of NO_3^- in roots drives long-distance transport of NO_3^- from roots to shoots in the *B. napus* (Xiangyou15). Inhibitor treatments of *B. napus* (Xiangyou15) hydroponics-grown plants were conducted at the seedling stage. Control: normal hydroponics solution; Bafi:(25 nmol·L^{-1}Bafilomycin A_1), an inhibitor of V-ATPase; DCCD:(10 μmol·L^{-1}DCCD + 50 mmol·$L^{-1}Na_2SO_3$), which together specifically inhibits V-PPase; and B+D: a 1:1 combination of Bafi and DCCD, which inhibits both V-ATPase and V-PPase. The inhibitors were applied at the seedling stage in hydroponic solutions for 24 h. Mature vacuoles were collected from the root tissues of the plant materials at the seedling stage. The NO_3^- flux measurement is described in the legend to Figure 1. Protoplasts and vacuoles isolated from roots of hydroponically grown plants were assessed for NO_3^- accumulation plotted as μmol NO_3^- per μmol *p*-nitrophenol as described in the legend to Figure 1 and in "Materials and Methods." Tonoplast proton-pump (V-ATPase and V-PPase) activities are shown in root tissues of *B. napus* as affected by inhibitor treatments (A). Different letters at the top of histogram bars denote significant differences in V-ATPase activities in root tissues between inhibitor treatments ($P < 0.05$); asterisks (*) at the top of the histogram bars denote significant differences in V-PPase activities in root tissues between inhibitor treatments ($P < 0.05$). Vertical bars on the figures indicate SD ($n = 6$). NO_3^- fluxes within the vacuoles of root tissues are shown for *B. napus* between inhibitor treatments (B). Different letters at the top of the histogram bars denote significant differences of NO_3^- flux between inhibitor treatments ($P < 0.05$). Vertical bars on the figures indicate SD ($n = 6$). Accumulation of NO_3^- inside the vacuole and in the protoplasts of root tissues is shown for *B. napus* (C). Values above the bars represent the percentage of vacuolar NO_3^- relative to the total NO_3^- in protoplasts. Vertical bars indicate

BnNRT1.8 decreased substantially (Fig. 4F). Similar results were also observed in Arabidopsis, where expression of *AtNRT1.5* in roots of the mutants (*vha-a2*, *vha-a3* and *avp1*) were significantly higher than in the wild type (col-0), but expression of *AtNRT1.8* in the same mutants were considerably lower (Fig. 5, E and F).

NO_3^- concentrations in the xylem sap, the N-distribution between shoot and root (S:R ratios based on [^{15}N]), and the [NO_3^-] in shoots relative to roots of the H genotype treated with energy pumps' inhibitors were significantly higher than in the control (Fig. 4, G and H; Supplemental Fig. S5A). Similar trends were also observed when using mutants of Arabidopsis deficient in the energy pumps' activities. NO_3^- concentration in the xylem sap, the [^{15}N] S:R ratios, and [NO_3^-] S:R ratios were all significantly higher in the mutants than in the wild type (Fig. 5, G and H; Supplemental Fig. S5B). These data clearly showed that prevention of N sequestration in vacuoles would enhance its translocation to shoot.

Additional evidence linking NO_3^- long-distance transport and NO_3^- short-distance distribution within cells were provided through experiments comparing Arabidopsis wild type (Ws) and mutant *clca-2* (Supplemental Fig. S6). The chloride channel (CLCa) is the main channel for vacuolar anion accumulation. Vacuolar sequestration capacity of NO_3^- significantly declines in *clca* mutants (De Angeli et al., 2006). NO_3^- influx into the vacuolar space of Ws roots was significantly higher than that observed in the *clca-2* mutants (Supplemental Fig. S6A). This resulted in a smaller proportion of vacuolar NO_3^- in *clca-2* plants relative to the total NO_3^- in root tissue protoplasts, as compared with Ws (Supplemental Fig. S6B). Consequently, the accumulation of NO_3^- in the cytosol was significantly higher in *clca-2* than in Ws plants (Supplemental Fig. S6C). The higher NO_3^- concentration in the cytosol together with the higher expression of *AtNRT1.5*, coupled with lower expression of *AtNRT1.8* in *clca-2* roots (Supplemental Fig. S6, D and E); resulted in significant increase in xylem sap NO_3^- concentration, [^{15}N] S:R ratios, and [NO_3^-] S:R ratios compared with Ws plants (Supplemental Fig. S6, F, G, and H).

Increased NO_3^- Translocation to Shoots Enhanced NUE

NO_3^- assimilation efficiency is known to be higher in shoots than in roots (Smirnoff and Stewart, 1985; Andrews, 1986; Tang et al., 2012, 2013). We therefore hypothesize that increased NO_3^- translocation to shoot and the consequent higher shoot:root ratio will contribute to higher NUE. Our data support this hypothesis. The H *B. napus* genotype showed enhanced long-distance transport of NO_3^- from roots to shoots (Fig. 2; Supplemental Fig. S2). This enhanced NO_3^- transport requires higher carbon skeleton provided through higher photosynthetic rate (Tang et al., 2012, 2013). Our results showed that chlorophyll content, intercellular CO_2 concentration, and photosynthetic rate were significantly higher in the H than the L genotype at both seedling and flowering stages (Table II). Moreover, the NO_3^- assimilating enzymes were strongly induced by NO_3^-, providing sufficient capacity for N assimilation (Smirnoff and Stewart, 1985; Andrews, 1986). NR and Gln synthetase (GS) activities in roots of the H genotype were significantly lower than in the L genotype both at seedling and flowering stages (Supplemental Fig. S7). In contrast, NR activities in shoots of the H genotype were significantly higher than in the L genotype at both stages (Supplemental Fig. S7, A and B); and GS activity in the H genotype was also higher than those of the L genotype at seedling stage (Supplemental Fig. S7C).

Experiments comparing Arabidopsis wild type (col-0, Ws) with mutants defective in vacuolar proton-pumps (*vha-a2*, *vha-a3*, *avp1*), and transport channel (*clca-2*) yielded similar results, that is, increases in NO_3^- shoot: root ratio essentially contributed to enhanced NUE (Fig. 6). The NO_3^- shoot:root ratios in Arabidopsis mutants were higher than that in the wild type (Fig. 5, G and H). Generally, the efficiency of inorganic N (NO_3^-) assimilation into organic N is higher in shoots than in roots (Smirnoff and Stewart, 1985; Andrews, 1986); therefore, the NO_3^- concentration in Arabidopsis mutants decreased (Fig. 6, C and D), leading to higher NUE compared with the wild type (Fig. 6, A and B).

BnNRT1.5/*BnNRT1.8* in *B. napus* Affects NO_3^- Long-Distance Transport from Roots to Shoots

Both *B. napus* and Arabidopsis are members of Cruciferae Family. The amino acid sequence identity between *BnNRT1.5* and *AtNRT1.5* was 90% (Supplemental Fig. S8A), and the amino acid sequence similarity between

Figure 4. (*Continued.*)
SD (n = 6). Accumulation of cytosolic NO_3^- in root tissues is shown for *B. napus* (D). P-V is the total NO_3^- in the cytosol; calculated as total NO_3^- in protoplasts − total NO_3^- in vacuoles. Different letters at the top of the histogram bars denote significant differences in total NO_3^- in vacuoles outside of the protoplast ($P < 0.05$). Vertical bars on the figures indicate SD (n = 6). Expression levels of the *BnNRT1.5* gene (E) and *BnNRT1.8*gene (F) are shown relative to that of the actin gene, assessed by quantitative RT-PCR as described in "Materials and Methods"; a value of 1.0 is equivalent to levels of expression of the *Bnactin* gene. Different letters at the top of the histogram bars denote significant differences in gene expression ($P < 0.05$). Vertical bars indicate SD (n = 3). Growth conditions for hydroponically grown plants with ^{15}N treatmen tare described in "Materials and Methods." The [^{15}N] S:R ratios as affected by inhibitor treatments are depicted for *B. napus* (G). The [NO_3^-] S:R ratio as affected by inhibitor treatments are shown for *B. napus* (H). Different letters at the top of the histogram bars denote significant differences ($P <$ 0.05). Vertical bars on the figures indicate SD (n = 3).

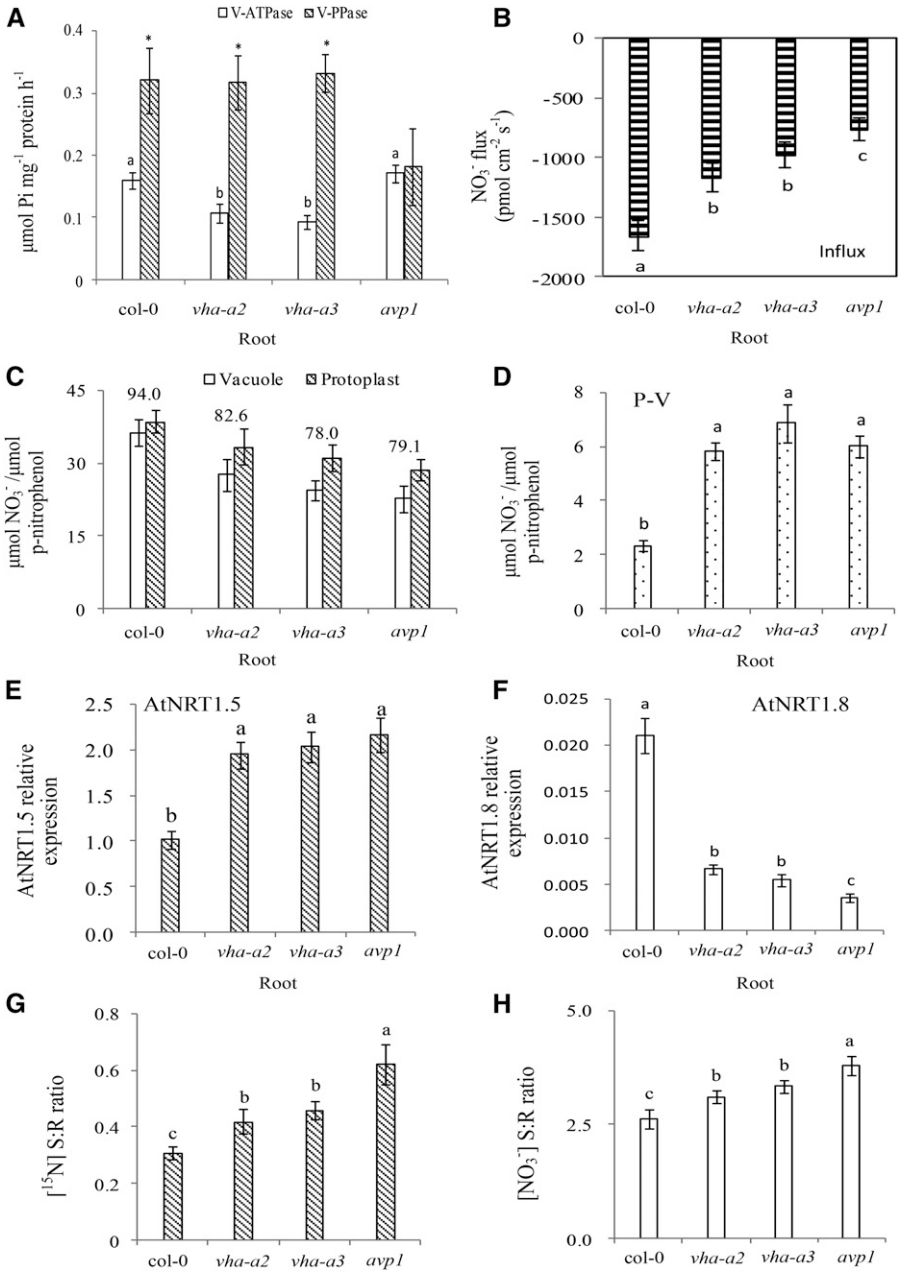

Figure 5. Reduced VSC of NO_3^- in roots drives long-distance transport of NO_3^- from roots to shoots in the Arabidopsis (col-0, *vha-a2, vha-a3, avp1*). Wild-type Arabidopsis plants (col-0), V-ATPase gene mutant plants (*vha-a2, vha-a3*), and V-PPase gene mutant plant (*avp1*) were used as the model plant materials. Mature vacuoles were collected from the root tissues of the plant materials at the seedling stage. The NO_3^- flux measurement is described in the legend to Figure 1. Protoplasts and vacuoles isolated from roots of hydroponically grown plants were assessed for NO_3^- accumulation plotted as μmol NO_3^- per μmol *p*-nitrophenol as described in the legend to Figure 1 and in "Materials and Methods." Tonoplast proton-pump (V-ATPase and V-PPase) activities are shown in root tissues from different Arabidopsis plant materials (A). Different letters at the top of the histogram bars denote significant differences in V-ATPase activities in root tissues between Arabidopsis plant materials ($P < 0.05$); asterisks (*) at the top of the histogram bars denote significant differences of V-PPase activities in root tissues ($P < 0.05$). Vertical bars indicate SD ($n = 6$). NO_3^- fluxes within the vacuoles of root tissues are shown for Arabidopsis between different mutants (B). Different letters at the top of the histogram bars denote significant differences in NO_3^- flux between Arabidopsis plant materials ($P < 0.05$). Vertical bars indicate SD ($n = 6$). Accumulation of NO_3^- inside the vacuole and in the protoplasts of root tissues is shown for Arabidopsis (C). Values above the bars represent the percentage of vacuolar NO_3^- relative to the total NO_3^- in protoplasts. Vertical bars indicate SD ($n = 6$). Accumulation of cytosol NO_3^- in root tissues is shown for Arabidopsis (D). P-V is the total NO_3^- in the cytosol; calculated as total NO_3^- in protoplasts – total NO_3^- in vacuoles. Different letters at the top of the histogram bars denote significant differences in total NO_3^- in the cytosol ($P < 0.05$). Vertical bars indicate SD ($n = 6$). Expression

Table II. *Variation inchlorophyll content, intercellular CO_2 concentration and photosynthetic rate between high and low nitrogen use efficiency genotypes of B. napus*

Different letters between the H and L genotypes denote a significant difference at $P < 0.05$ level. Data are means ± SD ($n = 6$).

Genotypes	Seedling stage			Flowering stage		
	Chlorophyll content[a](SP AD readings)	Intercellular CO_2 concentration (μmol $CO_2 mol^{-1}$)	Photosynthetic rate (μmol CO_2 m^{-2} s^{-1})	Chlorophyll content (SPAD readings)	Intercellular CO_2 concentration (μmol $CO_2 mol^{-1}$)	Photosynthetic rate (μmol CO_2 $m^{-2}s^{-1}$)
High	48.65 ± 1.29a	271.84 ± 7.64a	23.31 ± 0.96a	63.11 ± 2.08a	283.99 ± 20.84a	17.53 ± 0.58a
Low	45.86 ± 2.08b	246.36 ± 8.78b	21.02 ± 0.76b	57.40 ± 3.00b	233.68 ± 27.50b	16.22 ± 0.67b

[a]Chlorophyll content, intercellular CO_2 concentration, and photosynthetic rate were measured at 1000 h using a LI-6400 Portable Photosynthesis System. Measurements were conducted using the 4th leaf from the bottom at seedling stage and the 12th leaf from the bottom up at flowering.

BnNRT1.8 and *AtNRT1.8* was 90.8% (Supplemental Fig. S8B). Comparisons of nucleotide and amino acid sequences (Harper et al., 2012) of these genes (http://brassica.nbi.ac.uk/cgi-bin/microarray_database.cgi) showed that *BnNRT1.5* (EV220114) and *BnNRT1.8* (EV116423) of *B. napus* are, respectively, highly homologous with *AtNRT1.5* and *AtNRT1.8*, and the two genes are mainly expressed in roots of both species, showing similar organ-specificity (Lin et al., 2008; Li et al., 2010).

NO_3^- long-distance transport from roots to shoots is, therefore, regulated by *NRT1.5* and *NRT1.8*, as reported before (Lin et al., 2008; Li et al., 2010). The [^{15}N-traced] S:R ratios and the [NO_3^-] S:R ratios were significantly lower in *nrt1.5-3* mutants relative to the wild type (col-0), while [^{15}N] S:R and [NO_3^-] S:R ratios showed significant increase in *nrt1.8*-2 mutant relative to col-0 (Supplemental Fig. S9, C and D). A previous study showed that expression of *NRT1.5* is down-regulated by ACC and MeJA treatments, while the expression of *NRT1.8* is strongly up-regulated in Arabidopsis (Zhang et al., 2014). Consequently, NO_3^- accumulated in plant roots, probably as an adaptive measure for abiotic stresses (Chen et al., 2012). Both the H- and L- *B. napus* genotypes showed significantly lower expression of *BnNRT1.5* in roots when treated with ACC (Supplemental Fig. S10A), but the expression of *BnNRT1.8* remained higher than in the control plants (Supplemental Fig. S10B). This resulted in significantly lower [^{15}N] S:R ratios following ACC treatment (Supplemental Fig. S10, C, D, and E). These data indicate that *BnNRT1.5* and *BnNRT1.8* play similar functions for NO_3^- long-distance transport between root and shoot in both *B. napus* and Arabidopsis (Lin et al., 2008; Li et al., 2010).

DISCUSSION

Nitrate Long-Distance Transport from Root to Shoot Is Regulated by Cytosolic NO_3^- in Roots

NO_3^- long-distance transport from root to shoot is controlled by *NRT* gene family. For instance, xylem NO_3^- loading and unloading are mainly controlled by *NRT1.5* and *NRT1.8*, respectively (Lin et al., 2008; Li et al., 2010). Whereas the NO_3^- short-distance transport between the vacuole and cytosol is controlled by tonoplast proton pumps (V-ATPase and V-PPase; Krebs et al., 2010) and by activity of the CLCa channel in the tonoplast membrane (De Angeli et al., 2006; Wege et al., 2014), tonoplast proton pumps provide the energy required for NO_3^- accumulation into the vacuole through CLCa (Gaxiola et al., 2001; Brüx et al., 2008; Krebs et al., 2010). The expression of *NRT1.5* is up-regulated by NO_3^- in plant culture solution (Lin et al., 2008), whereas regulation of *NRT1.8* expression is contrary to that of *NRT1.5* under both control and abiotic stress conditions (Li et al., 2010; Chen et al., 2012; Zhang et al., 2014).

Despite the progress made in characterizing the genes involved in transport and metabolism of NO_3^- in plants, the relationship between long- and short-distance transport and how these two pathways are regulated has not been thoroughly investigated. We hypothesize that *NRT1.5* expression and its role in long-distance transport is regulated by NO_3^- in plant tissue as was observed in culture solution (Lin et al., 2008), and our data support this hypothesis. Both *BnNRT1.5* and *AtNRT1.5* expression were up-regulated by increasing cytosolic NO_3^- in roots (Figs. 4 and 5). The increase in cytosolic NO_3^- was achieved through (1) use of Arabidopsis mutants defective in proton pumps (V-ATPase and V-PPase) or CLCa activities in the tonoplast and (2) inhibition of *B. napus* tonoplast proton

Figure 5. (*Continued.*)
of the *AtNRT1.5* gene (E) and AtNRT1.8 gene (F) are shown relative to that of the actin gene, assessed by quantitative RT-PCR; a value of 1.0 is equivalent to levels of expression of the *Atactin2* gene. Different letters at the top of the histogram bars denote significant differences in gene expression ($P < 0.05$). Vertical bars on the figures indicate SD ($n = 3$). Growth conditions for hydroponically grown plants with ^{15}N treatment are described in "Materials and Methods." The [^{15}N] S:R ratios as affected by inhibitor treatments are depicted for various Arabidopsis mutants (G). The [NO_3^-] S:R ratio as affected by inhibitor treatments are depicted for various Arabidopsis mutants (H). Different letters at the top of the histogram bars denote significant differences ($P < 0.05$). Vertical bars on the figures indicate SD ($n = 3$).

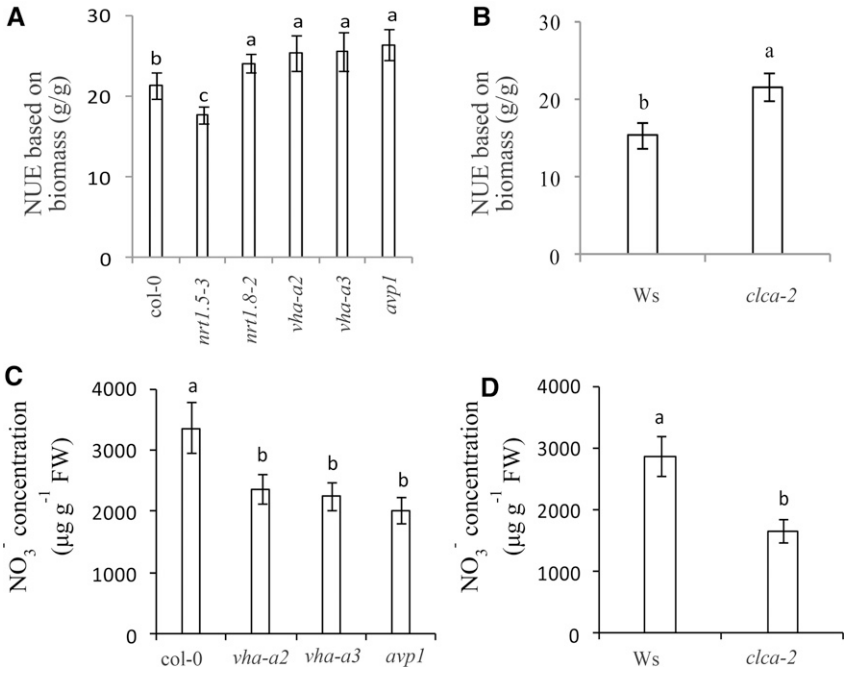

Figure 6. Increased NO_3^- shoots:roots ratio essentially contributed to enhancing NUE in Arabidopsis. Plants grown hydroponically were sampled for further analysis at seedling stage and at harvest. Conditions for hydroponics culture and characteristics of the various Arabidopsis genotypes are defined in "Materials and Methods." The wild-type Columbia-0 (col-0) plants were used as control for V-ATPase mutants (*vha-a2* and *vha-a3*), V-PPase mutants (*avp1*), *nrt1.5-3* mutants, and *nrt1.8-2* mutants; Arabidopsis wild-type Wassilewskija (Ws) plants were used as control for *clca-2* mutants. Differences in NUE based on biomass (A) and NO_3^- concentration (C) are shown for the wild-type (col-0) and mutants *nrt1.5-3*, *nrt1.8-2*, *vha-a2*, *vha-a3*, and *avp1*. Differences of NUE based on biomass (B) and NO_3^- concentration (D) are shown between Arabidopsis wild-type plants Ws and *clca-2*. Different letters at the top of the histogram bars denote significant differences between the Arabidopsis genotypes ($P < 0.05$). Vertical bars on the figures indicate SD ($n = 6$).

pumps. In both model plants, the influx of NO_3^- into vacuoles was substantially reduced, resulting in higher concentrations of NO_3^- in the cytosol (Fig. 4, A–D; Fig. 5, A–D; Supplemental Fig. S6, A–C). Under those conditions, expression of *BnNRT1.5* and *AtNRT1.5* was up-regulated by the enhanced cytosolic NO_3^-, while expression of *BnNRT1.8* and *AtNRT1.8* was down-regulated (Fig. 4, E and F; Fig. 5, E and F; Supplemental Fig. S6, D and E). As a consequence, more NO_3^- was loaded into the xylem sap and transported from root to shoot (Supplemental Fig. S5, A and B; Supplemental Fig. S6F). This is also reflected as increased shoot:root ratios of N, traced by [^{15}N] and [NO_3^-] (Fig. 4, G and H; Fig. 5, G and H; Supplemental Fig. S6, G and H).

Interestingly, the expression of both *BnNRT1.5* and *AtNRT1.5* is up-regulated by increased cytosolic NO_3^- concentration in roots, but were not affected by NO_3^- sequestered into vacuoles (Figs. 4 and 5; Supplemental Fig. S6). This is because vacuolar NO_3^- is functionally separated by the tonoplast and cannot be assimilated by enzymes that are localized in the cytosol. Therefore, NO_3^--inducible genes, such as NR and *NRT1.5*, were not influenced by vacuolar NO_3^- concentration (Martinoia et al., 1981; Martinoia et al., 2000; Zhang et al., 2012). In addition, NO_3^- concentration in the cytosol is controlled by its short-distance transport through the tonoplast, which is mediated through the tonoplast proton pumps, providing the required energy for its sequestration into vacuoles against concentration gradient (Gaxiola et al., 2001; Brüx et al., 2008; Krebs et al., 2010). The gradient of H^+ between the inside of the vacuole and the cytosol is maintained by an $2NO_3^-/^1H^+$ antiporter mechanism that facilitates, NO_3^- transport through CLCa (De Angeli et al., 2006; Wege et al., 2014). Our data provide clear evidence that NO_3^- long-distance transport from root to shoot is regulated by cytosolic NO_3^- concentration in roots.

Regulatory mechanisms that control the expression of *NRT1.8* and *NRT1.5* as mediated by NO_3^- are still unknown, however, previous studies showed that their expression is also affected by abiotic stresses, whereby *NRT1.5* is down-regulated and *NRT1.8* is up-regulated (Li et al., 2010; Zhang et al., 2014). *AtNRT1.8* expression in *Arabidopsis nrt1.5* mutants is highly up-regulated (Chen et al., 2012), as was also observed here (Fig. 3C). Moreover, *AtNRT1.5* expression was enhanced by NO_3^- in culture solution and was not affected in *nrt1.8-2* mutant (Fig. 3, A and B). On the other hand, *AtNRT1.8* expression was not affected by cytosolic NO_3^-, but down-regulated when *AtNRT1.5* expression was up-regulated by NO_3^-(Supplemental Fig. S6, D and E). Analogous results were also obtained with *B. napus* genotypes (Fig. 3, E and F). Based on these results we argue that *NRT1.8* expression is not directly influenced by cytosolic NO_3^-, but rather by *NRT1.5* expression (Figs. 4 and 5; Supplemental Fig. S6), suggesting *NRT1.8* is probably acting downstream of *NRT1.5*. Apparently the regulatory mechanisms of this *NRT* gene family still awaits further studies to be elucidated.

Response of NUE to NO_3^- Long-Distance Transport

NO_3^- assimilation efficiency is higher in shoot than in root tissues and can be further enhanced by carbon assimilation (Smirnoff and Stewart, 1985; Tang et al., 2013). Therefore, translocation of higher proportion of NO_3^- from roots to shoots likely contributes to better crop growth and higher NUE (Andrews, 1986; Tang et al., 2012). The current study provides direct evidence

for these results using contrasting *B. napus* genotype identified before (Zhang et al., 2009; Han et al., 2015a). Our data confirmed the genetic variation in NUE between these two genotypes (Table I).

We measured NO_3^- distribution in root and shoot of these genotypes to elucidate the physiological mechanisms contributing to variation in NUE. The data were consistent with our hypothesis that concentration of NO_3^- in the xylem sap and shoot would be significantly higher in the H genotype than in the L genotype (Fig. 2, E and F; Supplemental Fig. S2, E and F; Supplemental Fig. S4). The NO_3^- long-distance transport from root to shoot was affected by cytosolic NO_3^- in roots of both Arabidopsis and *B. napus* genotypes (Figs. 4 and 5; Supplemental Fig. S6). The activities of the tonoplast proton pumps in roots were significantly lower in the H genotype than in the L genotype (Fig. 1, A and B). Consequently, less NO_3^- was sequestered into the vacuole and more NO_3^- was retained in cytosol (Fig. 1, C and D). *BnNRT1.5* expression was then up-regulated, resulting in greater loading into the xylem, while *BnNRT1.8* was down-regulated (Fig. 2, A and B), probably to suppress NO_3^- unloading from xylem sap. Consequently, a higher proportion of NO_3^- was transported from root to shoots in the H genotype (Fig. 2, C and D; Supplemental Fig. S4).

Moreover, photosynthetic carbon fixation (Table II) and activities of both NR and GS were higher in shoots of the H genotype (Supplemental Fig. S7), both of which promote higher N assimilation. These results agreed with previous reports (Smirnoff and Stewart, 1985; Andrews, 1986; Tang et al., 2012; Tang et al., 2013), where higher NO_3^- transport from root to shoot, higher photosynthetic rate and N assimilation efficiency in shoots were suggested as essential mechanisms for high-NUE in crop plants. These qualities endowed the *B. napus* H genotype Xiangyou15 with higher NUE as compared with the L genotype, 814.

NO_3^- long-distance transport in *B. napus* is not only regulated by *BnNRT1.5* and *BnNRT1.8* in root tissues (Figs. 4 and 5; Supplemental Fig. S6), but also by stomatal conductance and transpiration, by indirectly controlling xylem sap flow and long-distance transport (Dechorgnat et al., 2011; Krapp et al., 2014). Stomatal conductance and transpiration rates of the H genotype were significantly higher than those of the L genotype (Supplemental Table S1), a result consistent with other studies describing characteristics of high-NUE plants (Daniel-Vedele et al., 1998; Wilkinson et al., 2007; Dechorgnat et al., 2011; Krapp et al., 2014).

Response of NUE to NO_3^- Short-Distance Transport

NUE is also strongly controlled by NO_3^- short-distance distribution between the vacuole and cytosol (Han et al., 2015a). A lower proportion of NO_3^- accumulating in vacuoles and a higher proportion retained in the cytosol will contribute to better NUE in crop plants (Han et al., 2015b). The energy required for vacuolar NO_3^- sequestration is provided by the tonoplast proton pumps (Gaxiola et al., 2001; Brüx et al., 2008; Krebs et al., 2010), while the distribution channel CLCa enables transport of NO_3^- across the vacuolar membrane (De Angeli et al., 2006; Wege et al., 2014). The activities of the tonoplast proton pumps (V-ATPase and V-PPase) in leaves of the H genotype were significantly lower than those of the L genotype at flowering stages (Han et al., 2015a, 2015b); thus, we expected similar differences in root tissues. Our results confirmed that the activities of tonoplast proton-pumps in root tissues of *B. napus* H genotype and Arabidopsis mutants were lower than those in the L genotype and Arabidopsis wild type, leading to less NO_3^- influx into vacuoles and more in the cytosol (Fig. 1; Fig. 5, A–D). Moreover, the enzymes catalyzing N assimilation are located in the cytoplasm where NO_3^- could be assimilated (Martinoia et al., 1981; Han et al., 2015a) or immediately loaded into xylem sap for long-distance transport from roots to shoots (Lin et al., 2008). Consequently, the NO_3^- concentration in root tissues of the H genotype and Arabidopsis mutants defective in tonoplast proton pumps was significantly lower than that in the L genotype (Fig. 2E) and in Arabidopsis wild type (Fig. 6C). Therefore, the higher proportion of NO_3^- transported to shoot and the lower concentrations retained in root vacuoles contributed to the higher NUE in Xiangyou15 and Arabidopsis mutants (*vha-a2*, *vha-a3*, and *avp1*; Table I; Fig. 6A). Further studies are needed to assess the impacts of regulating vacuolar sequestration of NO_3^- and rates of long-distance transport for enhancing NUE in other crop species and genotypes.

These data suggested that NO_3^- distribution between vacuoles and cytosol within cells regulates NO_3^- long-distance transport from root to shoot and ultimately affects NUE. NO_3^- loading into the xylem sap is an active transport process (Lin et al., 2008), therefore, not regulated by absolute concentration of NO_3^- in the cytosol but rather by genes involved in NO_3^- long-distance transport (*NRT1.5* and *NRT1.8*). Apparently, the expression of *NRT1.5*, the gene responsible for xylem loading is regulated by NO_3^-concentration in the cytosol.

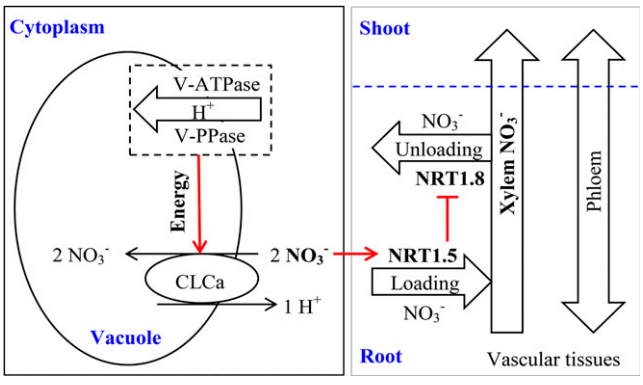

Figure 7. Simplified model for NO_3^- long-distance transport in xylem of vascular tissues. Long-distance transport is regulated by NO_3^- distribution between the vacuole and the cytosol in root tissues. Red lines display the route for regulation pathway.

Therefore, both NO_3^- short-distance transport across the tonoplast and its long-distance transport from root to shoot are important determinants of NUE in both *B. napus* and Arabidopsis (Table I; Fig. 6).

Roles of *NRT1.5* and *NRT1.8* in NO_3^- Long-Distance Transport in *B. napus* and Arabidopsis

Our results (Supplemental Figs. S9 and S10) showed that the proportion of NO_3^- distributed from root to shoot is strongly controlled by *NRT1.5*, in accord with previous studies (Lin et al., 2008; Li et al., 2010). The data suggest that the high-NUE genotypes possess lower activities of tonoplast proton-pumps (V-ATPase and V-PPase), resulting in less NO_3^- accumulation in vacuoles and more NO_3^- retention in cytosol (Fig. 7). The higher NO_3^- in the cytosol then up-regulated *NRT1.5*, which then down-regulates *NRT1.8*. As a result, more NO_3^- is loaded into the xylem system by *NRT1.5* mechanism, and less NO_3^- is unloaded via *NRT1.8* (Fig. 7). Differential regulation of these *NRT* genes in high-NUE plants increased transport of NO_3^- from root to shoot through the xylem vascular tissues (Fig. 7). This coordinated NO_3^- long- and short-distance transport likely fine-tunes NO_3^- allocation and modulates the balance of NO_3^- distribution between roots and shoots (Fig. 7).

Our research also revealed differences between Arabidopsis and *B. napus* in the expression of the wild-type *NRT* genes in response to NO_3^- in the protoplast. Moreover, using *A. thalianarnt1.5-3* mutants, we uncovered possible regulatory interactions between a functioning (wild-type) *NRT1.5* gene and *NRT1.8* expression in response to NO_3^- concentration. Because mutants defective in *nrt1.5* are not available for *B. napus*, we could not confirm that the respective *NRT1.5* and *NRT1.8* systems behave in an analogous way in these plant species. Based on Harper et al. (2012) research database, our homology comparisons and gene function annotations provided strong evidence for the roles of *BnNRT1.5* and *BnNRT1.8* in *B. napus*. Finally, our studies were conducted using two model dicotyledonous plant species, for which we had ample data on responses to specific inhibitors (*B. napus*), or specific mutants were available, with results forming the bases for the model presented in Figure 7. Further research using genetically diverse plant species (e.g. monocotyledonous crops such as rice, wheat, and corn), will help validate this model and its broader application across species. The information generated in this study could have future application for improving NUE in commercial crops, with consequent reduction in nitrogen use and benefits to the environment.

MATERIALS AND METHODS

Plant Material

The two oilseed rape (*B.napus*) cultivars used in this study have been characterized before as high (Xiangyou15, referred to as H genotype hereafter) and low (814, referred to as L genotype) NUE genotypes (Zhang et al., 2009; Han et al., 2015b). Here, we define NUE as the total biomass per unit of N uptake by the plant, with total biomass includes roots, shoots, and grains. The two genotypes were provided by the Hunan SubCenter of Improvement Center of National Oil Crops, Hunan, China.

The Arabidopsis (*Arabidopsis thaliana*) wild-type Columbia-0 (col-0) was used as control for V-ATPase (*vha-a2* and *vha-a3*), V-PPase (*avp1*), *nrt1.5-3*, and *nrt1.8-2* mutants, whereas the Arabidopsis wild-type Wassilewskija (Ws) was used as control for *clca-2* mutants. Arabidopsis mutants and transgenic lines (*nrt1.5-3* and *nrt1.8-2*) have been described previously (Chen et al., 2012; Zhang et al., 2014). The mutant lines *vha-a2* (Salk_142642) and *vha-a3* (Salk_122135) described by Krebs et al. (2010) were obtained from the Arabidopsis Biological Resources Center (ABRC). The mutant line *avp1* (GK-005004) described in Li et al. (2005) was obtained from the European Arabidopsis Stock Centre, while the mutant line *clca-2* (FST 171A06) described in De Angeli et al. (2006) was from the Institute National de la Recherche Agronomique (INRA) collection in France, together with the T-DNA mutants used for genotyping to select pure mutant lines.

Growth Conditions

B. napus plants were grown hydroponically in ceramic pots (20 cm × 15 cm) filled with a nutrient solution in the greenhouse under natural light as described in Han et al. (2015b). The pots were arranged in a completely randomized design with six biological replications. The nutrient solution was replaced every 3 d and its pH was adjusted to 5.5 daily. Experiments were conducted at the field station of Hunan Agricultural University, Southern China.

Arabidopsis plants were grown in a nutrient solution in plastic pots as described in Arteca and Arteca (2000) and Gong et al. (2003). The solution was changed every 3 d, with pH adjusted daily to 5.8. Pots were arranged in a completely randomized design with six biological replications. The nutrient solution used for both species consisted of 1.25 mM KNO_3, 0.625 mM KH_2PO_4, 0.5 mM $MgSO_4$, 0.5 mM Ca $(NO_3)_2 \cdot 4H_2O$, 0.025mM Fe-EDTA, 0.25 mlL^{-1} micronutrients (stock solution concentrations: 70 mM B, 14 mM Mn, 1 mM Zn, 0.5 mM Cu, and 0.2mM Mo). The experiments were conducted at Hunan Agricultural University in a phytotron set at 70% relative humidity, 16-h-light/8-h-dark cycle, and a constant temperature of 22°C.

Experimental Treatments and Phenotyping

All measurements made on *B. napus* plants were conducted either at the seedling stage (2 months after transplanting) or at flowering (5 months after transplanting). The whole root tissue was harvested and used for analyses at either stage. For shoot measurements, the fourth leaf from the bottom was used for measurements made at seedling stage, whereas the 12^{th} leaf from the bottom was harvested for measurements made at flowering stage. For Arabidopsis, whole root and shoot of 4-week-old plants were sampled and used for different assays.

Vacuolar Proton Pumps Inhibitor Treatments

Inhibition of vacuolar proton pumps of *B. napus* (Xiangyou15) was conducted at the seedling stage in hydroponic culture as described in Han et al. (2015a) with minor modifications. Plants grown in hydroponic solution were used as control. Inhibitor treatment was conducted using several chemicals: Bafi(25 nmol L^{-1} Bafilomycin A_1), an inhibitor of V-ATPase; DCCD(10 μmol L^{-1}DCCD + 50 $mmolL^{-1}$ Na_2SO_3), specifically inhibits V-PPase; and Bafi+DCCD in a 1:1 ratio as inhibitor of both V-ATPase and V-PPase. The inhibitors were applied in the hydroponic solutions for 24 h. Fresh plant tissue samples from all treatments were collected for different assays.

NO_3^- Induced Gene Expression

Four-week old Arabidopsis mutants (*nrt1.5-3*,*nrt1.8-2*) were grown in hydroponics with 2.25 mM $(NH_4)_2$ succinate for 3 d and shifted to hydroponics with 4.5 mM NO_3^- for 12 h; then root tissues were collected to assess relative expression of *AtNRT1.5* and *AtNRT1.8* genes. Seedlings of *B. napus* (Xiangyou15) plants grown hydroponically were treated with 5 mM $(NH_4)_2$ succinate for 3 d and shifted to fresh hydroponic solution containing 15 mM NO_3^- for 12 h. Root tissue was then collected to assess the relative expression of *BnNRT1.5* and *BnNRT1.8* genes using quantitative RT-PCR.

ACC Treatment

Hydroponically grown seedlings of *B. napus* were subjected to ACC treatment as described in Zhang et al. (2014) with minor modifications. Seedlings of the two genotypes Xiangyou15 and 814 were transferred to a nutrient solution containing 0.02mM L^{-1} ACC for 6 h or grown in normal hydroponic solution as control. Root tissues were then collected to assay relative expression of *BnNRT1.5* and *BnNRT1.8* using quantitative RT-PCR. Another set of *B. napus* plants were grown in ACC-containing hydroponic solution, but supplemented with $^{15}NO_3^-$ (22% ^{15}N) replacing the unlabeled NO_3^-, for 1 h. Root and shoot tissues were collected separately for ^{15}N measurement using a continuous-flow isotope ratio mass spectrometer coupled with a C-N elemental analyzer (ANCA-MS; PDZ Europa).

Biomass and N Concentration

Grain yield, dry biomass, and N concentration were determined in plant samples at harvest. Plants were harvested (including senescing leaves) then dried in an oven for 30 min at 105°C, then at 70°C to a constant weight and weighed. N concentration was determined using the Kjeldahl method (Shi et al., 2010; Han et al., 2015b); 0.2 g of dried samples were digested with H_2SO_4-H_2O_2 in a 100-mL Kjeldahl digestion flask, after which N concentration was determined using a Foss Auto Analyzer Unit (Kjeldahl 8400).

V-ATPase and V-PPase Activities

Roots (1.0 g) of *B. napus* were collected at seedling and flowering stages, and that of Arabidopsis (0.5 g) was sampled at seedling stage then used for determining the activities of V-ATPase and V-PPase (Han et al., 2015b). Activities of these two energy pumps within microsomal membranes were followed colorimetrically based on released Pi, as described by Zhu et al. (2001) and Krebs et al. (2010).

Assay of NO_3^- Flux in Vacuoles

Roots of both species were collected similarly as that used for V-ATPase and V-PPase activities, then used for vacuole isolation and measurement of NO_3^- flux in vacuoles as described by Robert et al. (2007), with minor modification (Han et al., 2015b). Net fluxes of NO_3^- in vacuoles were measured non-invasively using SIET (scanning ion-selective electrode technique, SIET system BIO-003A; Younger USA Science and Technology Corporation). An NO_3^--selective microelectrode used for the assay of NO_3^- flux was vibrated in the measuring solution between two positions, 1 μm and 11 μm from the vacuole surface (tonoplast), along an axis perpendicular to the tangent of the target vacuoles. Background signal was recorded by vibrating the electrode in the measuring solution in the absence of vacuoles. Ion flux was calculated by Fick's law of diffusion: $J = -D(dc/dx)$, where J represents the ion flux (picomolescm^{-2}s^{-1}), dc/dx is the ion concentration gradient, and D is the ion diffusion constant in a particular medium. The direction of the flux was derived from Fick's law of diffusion that relates the concentration gradient.

Isolation of Intact Protoplasts and Vacuoles for Determining NO_3^- Concentration

Similar to the above assays, root tissues (1.0 g) were collected from *B. napus* at seedling and flowering stages and from Arabidopsis (0.5 g) seedlings and used to isolate intact protoplasts and vacuoles as described by Robert et al. (2007), with minor modifications as outlined in Huang et al. (2012) and Han et al. (2015b). The purified protoplasts were divided into two equal aliquots, with one of them used for isolation of vacuoles. The purified protoplasts and vacuoles were then subsampled and used to determine NO_3^- concentrations (Vögeli-Lange and Wagner, 1990) and for enzyme activity assays (Ma et al., 2005). NO_3^- concentrations in protoplasts and vacuoles were measured by a continuous-flow auto-analyzer (Auto Analyzer 3, Bran and Luebbe) as described previously (Han et al., 2015b). The activities of acid phosphatase (ACP) and cytochrome oxidase (COX) were determined using plant ACP colorimetry and COX assay kits (GenMedSci Inc.) following the manufacturer's instructions. ACP activity specific to vacuoles was determined and used to normalize NO_3^- accumulation. We measured NO_3^- in the protoplast outside the vacuole, which includes the cytosol and organelles, e.g. mitochondria and Golgi Apparatus (Robert et al.2007). Since most of the NO_3^- in the protoplast outside the vacuole is located in the cytosol (Krebs et al., 2010), we refer to NO_3^- distribution between vacuoles and cytosol rather than vacuole versus protoplast.

Quantitative RT-PCR

Total RNA extracted from *B. napus* roots was prepared using Trizol reagent (Invitrogen). cDNAs were synthesized using M-MLV reverse transcriptase (Promega) following manufacturer's protocol. The relative expression of *BnNRT1.5* (EV220114), *BnNRT1.8* (EV116423), and *Bnactin* (AF111812.1) genes in plant roots were determined by quantitative RT-PCR and run on a Light-Cycler instrument (Roche) with the SYBR Green Real-Time PCR Master Mix Kit (TOYOBO) under the following conditions: 95°C for 2 min, then 45 cycles of 95°C for 10 s, 60°C for 10s and 72°C for 20 s. The primer sequences of *BnNRT1.5*, *BnNRT1.8*, and *Bnactin* genes were obtained from http://brassica.nbi.ac.uk as described in Harper et al. (2012), and expression levels were normalized to *Bnactin* as control.

Total RNA extracted from the 4-week-old Arabidopsis roots under the treatments conditions described above were prepared using Trizol reagent (Invitrogen). The cDNAs were synthesized using M-MLV reverse transcriptase (Promega) based on the manufacturer's protocol and as described in Li et al. (2010). The primer sequences of quantitative RT-PCR used in these assays are listed in Supplemental Table S2 and were described previously (Chen et al., 2012; Zhang et al., 2014), and their expression was normalized to *Atactin2* as control.

Determination of Nitrate Distribution Using $^{15}NO_3^-$

Hydroponically grown *B. napus* (seedling and flowering stages) and Arabidopsis (seedling) were transferred to 0.1 mM $CaSO_4$ solution for 1 min, then to their respective hydroponic nutrient solutions with $^{15}NO_3^-$ (22% excess) replacing unlabeled NO_3^- for 1h. Plants were then transferred to 0.1 mM $CaSO_4$ solution for 1 min, after which roots were washed with deionized water. Root and shoot samples were separated and dried at 105°C for 30 min, followed by 70°C for 3 d, then grounded and used for assaying ^{15}N content using a continuous-flow isotope ratio mass spectrometer coupled with a carbon-nitrogen elemental analyzer (ANCA-MS; PDZ Europa).

Xylem Sap Collection and Assay of Nitrate Concentration

We used the method of Tang et al. (2012) for collecting xylem sap. Plants were cut, leaving 1-cm segments with intact roots at seedling and flowering stages for *B. napus* and at seedling stage for Arabidopsis. Roots were immediately immersed in their respective nutrition solutions. Weighed cotton was put on the cut surface to absorb extruding xylem sap for 1 h. The cotton was then wrapped in plastic film and the volume of xylem sap was calculated as the weight gain of the cotton. Xylem sap was then squeezed from the cotton using a syringe and used for subsequent assay of nitrate concentration using a continuous-flow auto-analyzer (Auto Analyzer 3, Bran and Luebbe).

To determine nitrate concentration, samples (1.0 g fresh root and shoot at seedling and flowering of *B. napus* and 0.5 g fresh root and shoot of 4-week-old Arabidopsis) were frozen in liquid N_2 and ground with a mortar and pestle; the powder was then transferred to a beaker containing 70 ml deionized water and boiled for 30 min to extract nitrate, then cooled and made to 100 mL volume; and 0.2 g activated carbon was added to eliminate the effect of chlorophyll. The mixture was filtered, and nitrate in the filtrate was determined using a continuous-flow auto-analyzer (Auto Analyzer 3, Bran and Luebbe).

Measurements of Photosynthesis

All measurements of photosynthesis and related parameters were conducted at 1,000 h using intact leaves. The 4th leaf from the bottom in *B. napus* at seedling stage and the 12th leaf from the bottom at flowering stage were used for determining chlorophyll concentration, photosynthetic rate, intercellular CO_2 concentration, transpiration rate, and stomatal conductance. Chlorophyll concentration was determined by SPAD-502 (Minolta Camera Co., Ltd.; Luo et al., 2006; Yandeau-Nelson et al., 2011). Photosynthetic rate, intercellular CO_2 concentration, transpiration rate, and stomatal conductance were measured using LI-6400 Portable Photosynthesis System (Li-Cor Biosciences Co., Ltd.), set at flow rate of 500 μmol s^{-1}, photosynthetic photon flux density of 1000 μmol m^{-2} s^{-1}, relative humidity of 65%, CO_2 concentration of 400 ppm, and ambient temperatures.

NR and GS Activities

Leaves with similar age as those used for photosynthesis in *B. napus* were used for the assay of NR and GS activities. NR activity was measured by the modified method of Fan et al. (2007). Fresh samples (0.5 g) were frozen in liquid N_2, ground into powder in the presence of acid-washed sand and homogenized with 4 mL of extraction buffer (0.025mol L^{-1} phosphate buffer, pH 8.7, 1.211g L^{-1} Cys, 0.372g L^{-1} EDTA). Homogenates were centrifuged at 30,000 *g* for 15 min at 4°C, and the supernatants were treated with sulfanilamide and α-naphthylamine reagents for colorimetric (540 nm) determination of nitrite as described by Fan et al. (2007).

GS activity was determined using a modified reverseγ-glutamyltransferase method (Wang et al.2014), which measures the GS-catalyzed formation of glutamyl-γ-hydroxamate from Gln and hydroxylamine. Fresh samples were frozen for 30 min at −20°C, then ground in 10 mL Tris-HCl buffer and acid-washed sand. The homogenates were filtered through two layers of gauze and centrifuged at 8,000 *g* for 15 min at 4°C. About 1.2 mL of the supernatant was added in a reaction mixture and treated as described (Wang et al.2014). After the GS-catalyzed reaction was stopped and the solution was centrifuged, glutamyl-γ-hydroxamate was quantified colorimetrically in the supernatant (at 485 nm), and the concentration was determined using a standard curve.

Statistical Analyses

We used the SPSS software (Statistical Product and Service Solutions V13.0, USA) for ANOVA and mean separation of main effects and interactions using Duncan's multiple range test at $P < 0.05$. Values are presented as means and SD of three or six replicates from three independent experiments. Different letters or an asterisk (*) associated with specific data (e.g. at the top of histogram bars in figures or within tables) denote significant differences at $P < 0.05$.

Supplemental Data

The following supplemental materials are available.

Supplemental Figure S1. B. napus with higher NUE showed lower vacuolar sequestration capacity (VSC) for NO3− in roots at flowering stage.

Supplemental Figure S2. B. napus with higher NUE showed enhanced long-distance transport of NO3− from roots to shoots at flowering stage.

Supplemental Figure S3. The two B. napus (H and L genotypes) showed the same total N per plant at seedling stage (A) and flowering stage (B).

Supplemental Figure S4. B. napus with higher NUE showed increased NO3− concentration in the xylem sap at seedling and flowering stages.

Supplemental Figure S5. NO3- concentration in the xylem sap as affected by inhibitor treatments in B. napus and in the energy pumps' mutants of Arabidopsis (col-0, vha-a2, vha-a3, avp1).

Supplemental Figure S6. Reduced VSC for NO3− in roots drives long-distance transport of NO3− from roots to shoots in the Arabidopsis wild type (Ws) and mutant (clca-2).

Supplemental Figure S7. Differences of NR and GS activities between the two B. napus (H and L genotypes) at seedling and flowering stages.

Supplemental Figure S8. Amino acid sequences of BnNRT1.5 and BnNRT1.8.

Supplemental Figure S9. Functions of AtNRT1.5 and AtNRT1.8 genes in root tissues of Arabidopsis in controlling NO3- long-distance transport from root to shoots.

Supplemental Figure S10. B. napus BnNRT1.5 and BnNRT1.8 genes in roots were coordinately modulated to facilitate NO3- long distance transport from roots to shoots.

Supplemental Table S1. Differences in stomatal conductance and transpiration rate between the two B. napus genotypes.

Supplemental Table S2. Sequences of primers used for qRT-PCR.

ACKNOWLEDGMENTS

We thank Dr. Ji-Ming Gong (Shanghai Institute of Plant Physiology and Ecology, Shanghai Institutes for Biological Sciences) for providing *nrt1.5-3* and *nrt1.8-2* seeds.

Received December 9, 2015; accepted January 10, 2016; published January 12, 2016.

LITERATURE CITED

Andrews M (1986) The partitioning of nitrate assimilation between root and shoot of higher plants. Plant Cell Environ **9:** 511–519

Arteca RN, Arteca JM (2000) A novel method for growing *Arabidopsis thaliana* plants hydroponically. Physiol Plant **108:** 188–193

Brüx A, Liu TY, Krebs M, Stierhof YD, Lohmann JU, Miersch O, Wasternack C, Schumacher K (2008) Reduced V-ATPase activity in the trans-Golgi network causes oxylipin-dependent hypocotyl growth Inhibition in Arabidopsis. Plant Cell **20:** 1088–1100

Chen CZ, Lv XF, Li JY, Yi HY, Gong JM (2012) Arabidopsis *NRT1.5* is another essential component in the regulation of nitrate reallocation and stress tolerance. Plant Physiol **159:** 1582–1590

Chen X, Cui Z, Fan M, Vitousek P, Zhao M, Ma W, Wang Z, Zhang W, Yan X, Yang J, Deng X, Gao Q, et al (2014) Producing more grain with lower environmental costs. Nature **514:** 486–489

Chiu CC, Lin CS, Hsia AP, Su RC, Lin HL, Tsay YF (2004) Mutation of a nitrate transporter, AtNRT1:4, results in a reduced petiole nitrate content and altered leaf development. Plant Cell Physiol **45:** 1139–1148

Chopin F, Orsel M, Dorbe MF, Chardon F, Truong HN, Miller AJ, Krapp A, Daniel-Vedele F (2007) The Arabidopsis *ATNRT2.7* nitrate transporter controls nitrate content in seeds. Plant Cell **19:** 1590–1602

Daniel-Vedele F, Filleur S, Caboche M (1998) Nitrate transport: a key step in nitrate assimilation. Curr Opin Plant Biol **1:** 235–239

De Angeli A, Monachello D, Ephritikhine G, Frachisse JM, Thomine S, Gambale F, Barbier-Brygoo H (2006) The nitrate/proton antiporter *AtCLCa* mediates nitrate accumulation in plant vacuoles. Nature **442:** 939–942

Dechorgnat J, Nguyen CT, Armengaud P, Jossier M, Diatloff E, Filleur S, Daniel-Vedele F (2011) From the soil to the seeds: the long journey of nitrate in plants. J Exp Bot **62:** 1349–1359

Fan SC, Lin CS, Hsu PK, Lin SH, Tsay YF (2009) The Arabidopsis nitrate transporter *NRT1.7*, expressed in phloem, is responsible for source-to-sink remobilization of nitrate. Plant Cell **21:** 2750–2761

Fan X, Jia L, Li Y, Smith SJ, Miller AJ, Shen Q (2007) Comparing nitrate storage and remobilization in two rice cultivars that differ in their nitrogen use efficiency. J Exp Bot **58:** 1729–1740

Gaxiola RA, Li J, Undurraga S, Dang LM, Allen GJ, Alper SL, Fink GR (2001) Drought- and salt-tolerant plants result from overexpression of the *AVP1* H^+-pump. Proc Natl Acad Sci USA **98:** 11444–11449

Glass ADM, Britto DT, Kaiser BN, Kinghorn JR, Kronzucker HJ, Kumar A, Okamoto M, Rawat S, Siddiqi MY, Unkles SE, Vidmar JJ (2002) The regulation of nitrate and ammonium transport systems in plants. J Exp Bot **53:** 855–864

Gong JM, Lee DA, Schroeder JI (2003) Long-distance root-to-shoot transport of phytochelatins and cadmium in *Arabidopsis*. Proc Natl Acad Sci USA **100:** 10118–10123

Granstedt RC, Huffaker RC (1982) Identification of the leaf vacuole as a major nitrate storage pool. Plant Physiol **70:** 410–413

Han YL, Liao Q, Yu Y, Song HX, Liu Q, Rong XM, Gu JD, Lepo JE, Guan CY, Zhang ZH (2015a) Nitrate reutilization mechanisms in the tonoplast of two *Brassica napus* genotypes with different nitrogen use efficiency. Acta Physiol Plant **37:** 42

Han YL, Liu Q, Gu JD, Gong JM, Guan CY, Lepo JE, Rong XR, Song HX, Zhang ZH (2015b) V-ATPase and V-PPase at the Tonoplast affect NO_3^- Content in *Brassica napus* by Controlling Distribution of NO_3^- between the Cytoplasm and Vacuole. J Plant Growth Regul **34:** 22–34

Harper AL, Trick M, Higgins J, Fraser F, Clissold L, Wells R, Hattori C, Werner P, Bancroft I (2012) Associative transcriptomics of traits in the polyploid crop species Brassica napus. Nat Biotechnol **30:** 798–802

Huang J, Zhang Y, Peng JS, Zhong C, Yi HY, Ow DW, Gong JM (2012) Fission yeast *HMT1* lowers seed cadmium through phytochelatin-dependent vacuolar sequestration in *Arabidopsis*. Plant Physiol **158:** 1779–1788

Krapp A, David LC, Chardin C, Girin T, Marmagne A, Leprince AS, Chaillou S, Ferrario-Méry S, Meyer C, Daniel-Vedele F (2014) Nitrate transport and signalling in Arabidopsis. J Exp Bot **65:** 789–798

Krebs M, Beyhl D, Gorlich E, Al-Rasheid KA, Marten I, Stierhof YD, Hedrich R, Schumacher K (2010) Arabidopsis V-ATPase activity at the tonoplast is required for efficient nutrient storage but not for sodium accumulation. PNAS **107:** 3251–3256

Lin SH, Kuo HF, Canivenc G, Lin CS, Lepetit M, Hsu PK, Tillard P, Lin HL, Wang YY, Tsai CB, Gojon A, Tsay YF (2008) Mutation of the *Arabidopsis NRT1.5* nitrate transporter causes defective root-to-shoot nitrate transport. Plant Cell **20:** 2514–2528

Li JY, Fu YL, Pike SM, Bao J, Tian W, Zhang Y, Chen CZ, Zhang Y, Li HM, Huang J, Li LG, Schroeder JI, et al (2010) The *Arabidopsis* nitrate transporter *NRT1.8* functions in nitrate removal from the xylem sap and mediates cadmium tolerance. Plant Cell **22:** 1633–1646

Li J, Yang H, Peer WA, Richter G, Blakeslee J, Bandyopadhyay A, Titapiwantakun B, Undurraga S, Khodakovskaya M, Richards EL, Krizek B, Murphy AS, et al (2005) *Arabidopsis* H^+-PPase *AVP1* regulates auxin-mediated organ development. Science **310:** 121–125

Luo JK, Sun SB, Jia LJ, Chen W, Shen QR (2006) The mechanism of nitrate accumulation in Pakchoi. *Brassica campestris*L.ssp.*Chinensis* (L.). Plant Soil **282:** 291–300

Ma JF, Ueno D, Zhao FJ, McGrath SP (2005) Subcellular localisation of Cd and Zn in the leaves of a Cd-hyperaccumulating ecotype of Thlaspi caerulescens. Planta **220:** 731–736

Martinoia E, Massonneau A, Frangne N (2000) Transport processes of solutes across the vacuolar membrane of higher plants. Plant Cell Physiol **41:** 1175–1186

Martinoia E, Heck U, Wiemken A (1981) Vacuoles as storage compartments for nitrate in barley leaves. Nature **289:** 292–294

Miller AJ, Smith SJ (2008) Cytosolic nitrate ion homeostasis: could it have a role in sensing nitrogen status? Ann Bot (Lond) **101:** 485–489

Robert S, Zouhar J, Carter C, Raikhel N (2007) Isolation of intact vacuoles from *Arabidopsis* rosette leaf-derived protoplasts. Nat Protoc **2:** 259–262

Schroeder JI, Delhaize E, Frommer WB, Guerinot ML, Harrison MJ, Herrera-Estrella L, Horie T, Kochian LV, Munns R, Nishizawa NK, Tsay YF, Sanders D (2013) Using membrane transporters to improve crops for sustainable food production. Nature **497:** 60–66

Shi WM, Xu WF, Li SM, Zhao XQ, Dong GQ (2010) Responses of two rice cultivars differing in seedling-stage nitrogen use efficiency to growth under low-nitrogen conditions. Plant Soil **326:** 291–302

Shen QR, Tang L, Xu YC (2003) A review on the behavior of nitrate in vacuoles of plants. Acta Pedologica Sinica **40:** 465–470.

Smirnoff N, Stewart G (1985) Nitrate assimilation and translocation by higher plants: Comparative physiology and ecological consequences. Physiol Plant **64:** 133–140

Tang Y, Sun X, Hu C, Tan Q, Zhao X (2013) Genotypic differences in nitrate uptake, translocation and assimilation of two Chinese cabbage cultivars [Brassica campestris L. ssp. Chinensis (L.)]. Brassica campestris L. ssp. Chinesnsis. L. Plant Physiol Biochem **70:** 14–20

Tang Z, Fan X, Li Q, Feng H, Miller AJ, Shen Q, Xu G (2012) Knockdown of a rice stelar nitrate transporter alters long-distance translocation but not root influx. Plant Physiol **160:** 2052–2063

Vögeli-Lange R, Wagner GJ (1990) Subcellular localization of cadmium and cadmium-binding peptides in tobacco leaves : implication of a transport function for cadmium-binding peptides. Plant Physiol **92:** 1086–1093

Wang G, Ding G, Li L, Cai H, Ye X, Zou J, Xu F (2014) Identification and characterization of improved nitrogen efficiency in interspecific hybridized new-type *Brassica napus*. Ann Bot (Lond) **114:** 549–559

Wang YY, Tsay YF (2011) *Arabidopsis* nitrate transporter *NRT1.9* is important in phloem nitrate transport. Plant Cell **23:** 1945–1957

Wege S, De Angeli A, Droillard MJ, Kroniewicz L, Merlot S, Cornu D, Gambale F, Martinoia E, Barbier-Brygoo H, Thomine S, Leonhardt N, Filleur S (2014) Phosphorylation of the vacuolar anion exchanger *AtCLCa* is required for the stomatal response to abscisic acid. Sci Signal **7:** ra65

Wilkinson S, Bacon MA, Davies WJ (2007) Nitrate signalling to stomata and growing leaves: interactions with soil drying, ABA, and xylem sap pH in maize. J Exp Bot **58:** 1705–1716

Xu G, Fan X, Miller AJ (2012) Plant nitrogen assimilation and use efficiency. Annu Rev Plant Biol **63:** 153–182

Yandeau-Nelson MD, Laurens L, Shi Z, Xia H, Smith AM, Guiltinan MJ (2011) Starch-branching enzyme IIa is required for proper diurnal cycling of starch in leaves of maize. OA. Plant Physiol **156:** 479–490

Zhang GB, Yi HY, Gong JM (2014) The Arabidopsis ethylene/jasmonic acid-NRT signaling module coordinates nitrate reallocation and the trade-off between growth and environmental adaptation. Plant Cell **26:** 3984–3998

Zhang ZH, Song HX, Qing L, Rong XM, Xie GX, Peng JW, Zhang YP (2009) Study on differences of nitrogen efficiency and nitrogen response in different oilseed rape (*Brassica napus* L.) varieties. Asian Journal of Crop Science **1:** 105–112

Zhang ZH, Song HX, Liu Q, Rong XM, Peng JW, Xie GX, Zhang YP, Guan CY (2010) Nitrogen redistribution characteristics of oilseed rape varieties with different nitrogen use efficiencies during later growth period. Commun Soil Sci Plant Anal **41:** 1693–1706

Zhang ZH, Huang HT, Song HX, Liu Q, Rong XM, Peng JW, Xie GX, Zhang YP, Guan CY (2012) Research advances on nitrate nitrogen reutilization by proton pump of tonoplast and its relation to nitrogen use efficiency. Australian Journal of Crop Science **6:** 1377–1382

Zhu ZJ, Qian YR, Pfeiffer W (2001) Effect of nitrogen form on the activity of tonoplast pyrophosphatase in tomato roots. Acta Bot Sin **43:** 1146–1149